Electronic Supplementary Information

An "Active Site Anchoring" Strategy for the Preparation of PBO Fiber Derived Carbon Catalyst with Efficient Oxygen Reduction Reaction and Zinc-Air Batteries

Weihua Zhong[a,b], Zuoxu Xiao[b], Yunjun Luo[a,*], Dianbo Zhang[b], Xiangdong Chen[b], Jinwang Bai[b]

[a] *School of Materials Science & Engineering, Beijing Institute of Technology, 100081, Beijing, China*

[b] *Shandong Institute of Nonmetallic Materials, Jinan, 250031, Shandong, China*

Characterization

Raman spectra were carried out on a laser Raman microscope system (HORIBA Evolution Raman scope) with the excitation wavelength of 532 nm. X-ray diffraction patterns were performed on a Rigaku UItima IV X-Ray Diffractometer. FESEM images were observed on field-emission scanning electron microscope (SEM, Quant 250FEG). High-resolution transmission electron microscopy images were collected at an acceleration voltage of 200 kV (TEM, JEM-2100F).

Electrochemical measurements

The electrochemical measurements were evaluated using a CHI660E electrochemical work station in a standard three-electrode setup with a glass carbon electrode loaded with the catalysts was used as the working electrode. The procedure for the preparation of a working electrode was as following: 5 mg of the catalyst powder was dispersed in 800 μL of absolute ethanol and 30 μL of Nafion to obtain a homogeneous ink under ultrasonication, then 10 μL of the ink was slightly dropped on the working electrode. For ORR tests, cyclic voltammetry (CV) curves were tested in a N_2-saturated or O_2-saturated 0.1 M KOH electrolyte with a scan rate of 50 mV s^{-1}. RDE tests was measured in O_2-saturated 0.1 M KOH electrolyte at 10 mV s^{-1}.

Zinc-air battery tests:

The measurements of zinc-air batteries were evaluated under ambient conditions. A polished zinc plate and 6.0 M KOH solution were used as anode and electrolyte, respectively. The cathode was prepared by loading catalysts on the carbon paper (catalyst loading amount of 1.0 mg cm^{-2}).
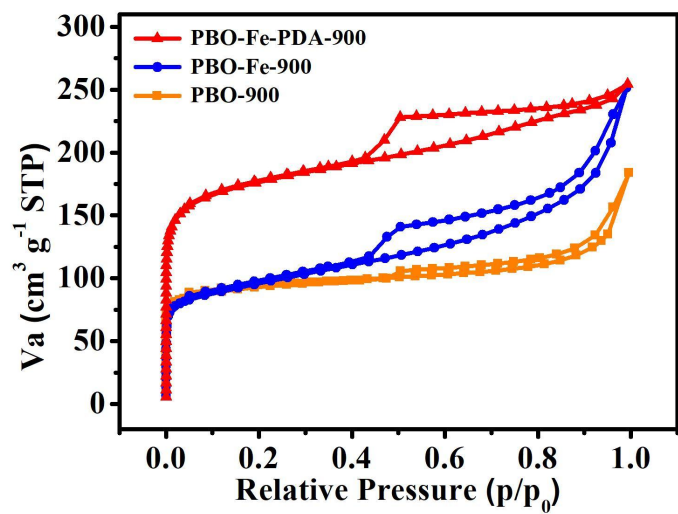
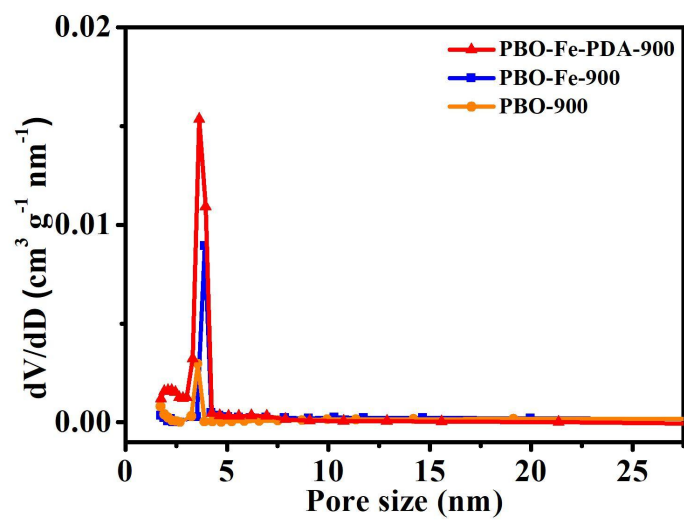**Fig. S1.** Nitrogen adsorption/desorption curves of PBO-900, PBO-Fe-900 and PBO-Fe-PDA-900.

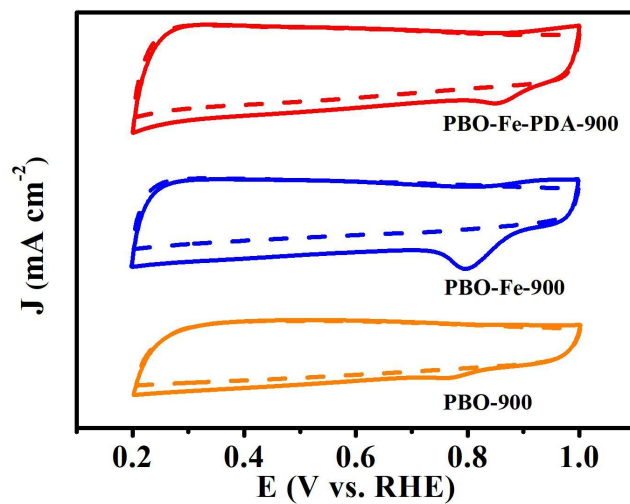**Fig. S2.** Pore size distributions of PBO-900, PBO-Fe-900 and PBO-Fe-PDA-900.

Fig. S3. CV curves of PBO-900, PBO-Fe-900 and PBO-Fe-PDA-900 in O_2-saturated (solid lines) and N_2-saturated (dot lines) 0.1 M KOH at 50 mV s^{-1}, respectively.
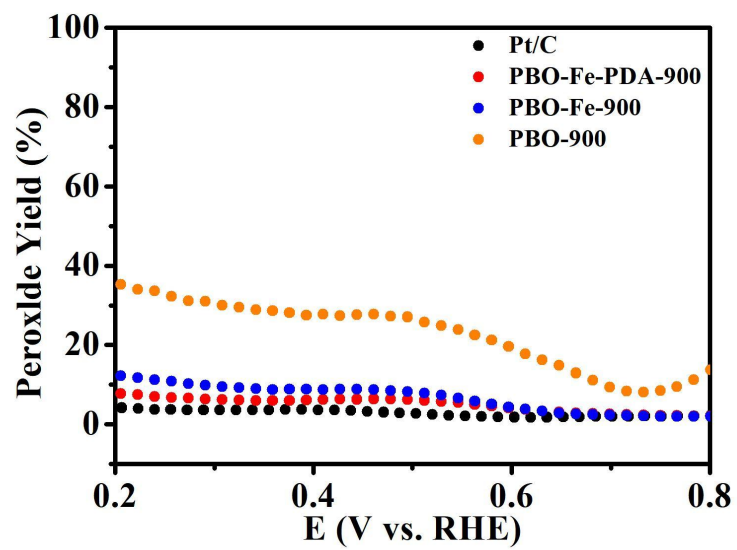
Fig. S4. Peroxide yield of the comparative catalysts.

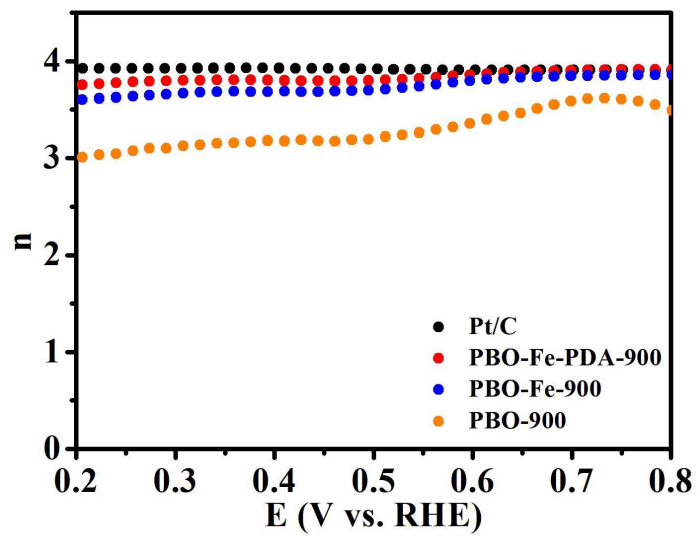**Fig. S5.** Transferred electron number of the comparative catalysts.
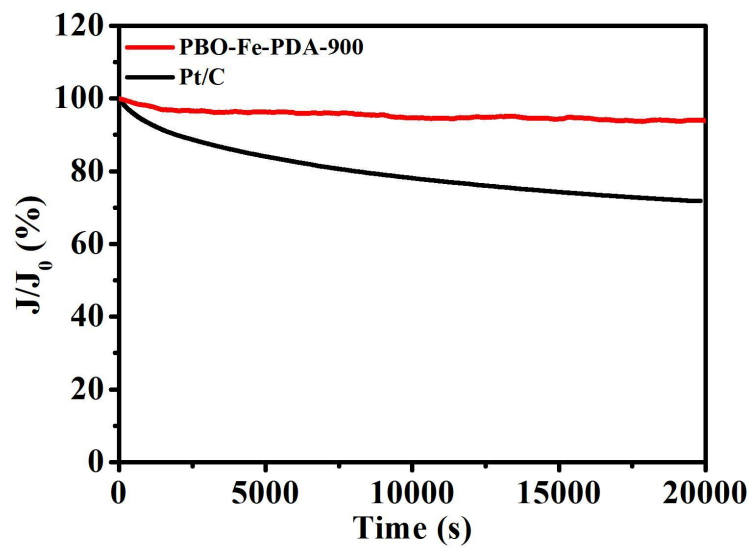
Fig. S6. Amperometric i-t curves of PBO-Fe-PDA-900 and wt% Pt/C.

Table S1. Comparison of the ORR performance for PBO-Fe-PDA-900 and other non-noble metal-based catalysts in 0.1 M KOH.

Catalyst	$E_{1/2}$/V	Tafel Slope/mV dec^{-1}	catalytic stability	Reference
PBO-Fe-PDA-900	0.86	73	93% (20000 S)	This Work
N-rich Fe-NC	0.78	70.72	98.3% (7200 S)	J. Alloys Compd. 2021, 884
Cu-Fe-N-C	0.86	100.1	/	Appl. Catal. B-Environ. 2019, 242: 209-217
Fe$_3$C-C	0.82	73.9	85% (30000 S)	ACS Appl. Nano Mater. 2021, 4: 8360-8367
FeNC-900	0.848	61.4	92% (30000 S)	Carbon 2019, 154:466-477
Fe$_3$O$_4$/N-CNTs	0.804	/	94% (20000 S)	Int. J. Hydrogen Energy, 2022, 47: 20529-20539
Fe-N-S-CNS	0.829	60.4	94.3% (50000 S)	Chem Eng J, 2021, 420: 127601.
Co-Ni (trace)/NCNTs	0.83	/	97.8% (20000 S)	Int. J. Hydrogen Energy, 2022, 47: 7761-7769

Fe/NPCF-900a	0.83	85	83.6% (50000 S)	Nanoscale. 2019, 11, 10257-10265